

## 光学学报

基于声致光纤光栅输出1.1~1.5  $\mu\text{m}$  波段高功率随机涡旋光束李阳<sup>1</sup>, 姚天甫<sup>1,2,3\*</sup>, 范晨晨<sup>1</sup>, 郝修路<sup>1</sup>, 马小雅<sup>1</sup>, 许将明<sup>1</sup>, 张青松<sup>4</sup>, 曾祥龙<sup>4\*\*</sup>, 周朴<sup>1</sup><sup>1</sup>国防科技大学前沿交叉学科学院, 湖南 长沙 410073;<sup>2</sup>国防科技大学南湖之光实验室, 湖南 长沙 410073;<sup>3</sup>高能激光技术湖南省重点实验室, 湖南 长沙 410073;<sup>4</sup>上海大学特种光纤与光接入网重点实验室, 特种光纤与先进通信国际合作联合实验室, 上海 200444

**摘要** 近年来,携带轨道角动量(OAM)的涡旋光束因具有重要研究价值和应用前景而备受关注。随着涡旋光束在传感、测量以及大容量光通信中的应用,输出带宽以及波长可调谐性成为关注的热点。突破稀土掺杂光纤发射波长限制和宽带模式转换的器件是实现特殊波段/宽带涡旋光输出的基础。为同时满足以上要求,本文采用基于分布式瑞利散射的随机拉曼光纤激光器结构,结合具备宽带模式转换能力的声致光纤光栅(AIFG),通过级联拉曼频移,实现了1133.9、1197.6、1260.5、1331.8、1414.5、1513.7 nm波长处拓扑荷数 $l=\pm 1$ 的涡旋光束输出,并通过自干涉实验进行验证。在1513.7 nm波长处功率为23.6 W,效率为31.1%。该研究不仅在全光纤中实现了紧凑的波长可调谐高功率涡旋光输出,验证了AIFG的超宽模式转换能力,也为其他波段涡旋光输出提供了参考方案,可进一步拓展涡旋光在多维光通信、光场与物质相互作用等领域的应用。

**关键词** 随机拉曼光纤激光器; 涡旋光束; 声致光纤光栅; 轨道角动量

中图分类号 TN248

文献标志码 A

DOI: 10.3788/AOS240432

## 1 引言

近年来,携带轨道角动量(OAM)的涡旋光束备受关注。涡旋光束具有螺旋型相位波前,中心为相位奇点,光强呈环形中空分布,同时每个光子携带 $l\hbar$ 的OAM,其中 $l$ 为拓扑荷数,涡旋面的方向取决于 $l$ 的正负。涡旋光束独特的物理性质使其在光通信<sup>[1]</sup>、粒子加速<sup>[2]</sup>、微粒操控<sup>[3]</sup>、超分辨成像<sup>[4]</sup>、激光与物质相互作用<sup>[5]</sup>等领域具有广泛的应用前景。目前,产生涡旋光场的方式主要分为两类:一类是空间结构产生,例如通过超表面<sup>[6]</sup>、空间光调制器<sup>[7]</sup>、螺旋相位板<sup>[8]</sup>、q-波片<sup>[9]</sup>等;另一类是光纤中产生,主要依靠少模光纤光栅<sup>[10]</sup>、长周期光纤光栅<sup>[11-12]</sup>、光子灯笼<sup>[13]</sup>、模式选择耦合器<sup>[14]</sup>、声致光纤光栅<sup>[15-18]</sup>等光纤模式转换器件。基于光纤产生的涡旋光束稳定性更佳,且与光通信系统兼容,利于集成和降低成本,近年来得到广泛发展<sup>[19]</sup>。此外,基于阵列激光相干合成<sup>[20-21]</sup>产生的涡旋光束,在高功率放大以及切换速度上具备显著优势。

值得注意的是,受限于稀土掺杂光纤增益带宽,目前涡旋光束输出主要集中在1  $\mu\text{m}$ 和1.5  $\mu\text{m}$ 等近红外

波段以及可见光波段。随着涡旋光束在传感、测量以及大容量光通信中的应用,涡旋光束的输出带宽以及波长可调谐性成为关注的热点。多个课题组对涡旋光束的波长可调谐性进行了研究。上海大学基于手性长周期光纤光栅,在1.5  $\mu\text{m}$ 波段实现了 $l=\pm(1\sim 3)$ 的涡旋光束输出,波长调谐范围约20 nm<sup>[12]</sup>。上海理工大学采用涡旋波片作为模式转换器件,结合衍射光栅实现波长调谐,实现了1015~1038 nm波长的 $l=\pm 1$ 的涡旋脉冲输出<sup>[22]</sup>。厦门大学通过445 nm激光二极管泵浦镨铈共掺的ZBLAN光纤,在红光波段实现涡旋光和柱矢量光输出,并通过改变Sagnac环境的工作波长,实现了633.89~636.02 nm波长可调<sup>[23]</sup>。近期,北京邮电大学提出了一种等离激元超构表面辅助的波长可调谐拓扑荷数 $l=\pm 1$ 的涡旋光束激光器,在1  $\mu\text{m}$ 波段波长调谐范围为60 nm<sup>[24]</sup>,该系统为空间结构,输出功率为5 mW,激光器效率低于10%。

以上波长可调谐的方案虽然在一定程度上填补了涡旋光束波长空白,但调谐范围较小,输出激光波长仍处于稀土离子发射波段中。拉曼激光技术是在更宽波段实现波长可调谐的重要方案。基于无源光纤受激拉

收稿日期: 2024-01-02; 修回日期: 2024-03-15; 录用日期: 2024-03-21; 网络首发日期: 2024-04-01

基金项目: 国家自然科学基金(12174445, 62061136013)

通信作者: \*yaotianfumary@163.com; \*\*zenglong@shu.edu.cn

曼散射产生频移,理论上只要有合适的泵浦源,就可以实现传输波段内任意波长的激光输出<sup>[25]</sup>。近期,本课题组基于声致光纤光栅(AIFG),在全光纤拉曼振荡器中实现了 1134 nm 处  $l=\pm 1$  的连续波涡旋光输出,最高功率达到 70 W<sup>[18]</sup>。Wu 等<sup>[26]</sup>通过 1545 nm 激光器泵浦,采用自制的模式选择耦合器结合偏振控制,在耗散孤子共振全光纤拉曼光纤激光器中产生涡旋光束。近年来,基于分布式瑞利散射的随机拉曼光纤激光器由于具有结构简单、时序稳定、相干性低等优点,得到广泛研究<sup>[27-28]</sup>;同时,分布式瑞利散射具有宽带特性,在波长捷变和宽带可调方面具有显著优势。Ma 等<sup>[29]</sup>基于空间光调制器,实现了瓦级涡旋随机拉曼激光,波长为 1092.1 nm,拓扑荷可实现  $-50\sim+50$  的切换。Luo 等<sup>[30]</sup>通过随机激光器的级联拉曼频移,实现了从 976 nm 的泵浦光到 1403 nm 波长信号光转换,并基于数字微镜器件(DMD)在腔外生成了涡旋光束,但激光器效率低于 6%,且复杂的空间光路增加了系统不稳定性。

为在全光纤结构中拓宽涡旋光束波长范围,还需要宽带的光纤模式转换器件,目前光纤模式转换器件中,少模光纤光栅、长周期光纤光栅、光子灯笼、模式选择耦合器等,往往是根据激光目标波长进行参数设计和制作,其调谐范围十分有限。AIFG 通过无源光纤中的声光耦合实现模式转换,当工作波长变化时,只须改变加载在 AIFG 上电信号频率,而无须对模式转换器件参数进行重新设计和替换,理论上具备极宽工作带宽<sup>[15-18]</sup>。因此,本文选择 AIFG 作为模式转换器件。与文献[18]所用的 AIFG 相比,本文采用的 AIFG 进一步优化了声光作用距离、压电陶瓷种类以及光纤类型等,实现了作用波长的进一步拓宽。

本文将 AIFG 结合级联随机拉曼光纤激光器,在全光纤系统中通过多级拉曼频移转换输出波长。实验中泵浦光为 1080 nm,通过多级频移,分别实现了 1133.9、1197.6、1260.5、1331.8、1414.5、1513.7 nm 波长处拓扑荷数  $l=\pm 1$  的涡旋光束输出,并通过自干涉实验验证了拓扑荷数,在 6 级转换后,1513.7 nm 波长处

功率为 23.6 W,效率为 31.1%。该实验不仅验证了 AIFG 超宽的模式转换特性,也为其他波段涡旋光输出提供了参考方案,可进一步拓展涡旋光在多维光通信、光场与物质相互作用等领域的应用。

## 2 实验装置和原理

### 2.1 AIFG 工作原理及特性

本文实验基于自制的 AIFG 实现波长可调谐的涡旋光输出。AIFG 由压电陶瓷(PZT)、射频(RF)信号源和少模光纤(FMF)(YOFC FM SI-2-ULL)构成。射频信号源产生的电信号加载至 PZT, PZT 将以与所施加信号相同的频率振动产生声波并传输至剥去涂覆层的 FMF 中。周期性的声致振动将在光纤中传播,最终形成类似于长周期光纤光栅的折射率调制,光栅周期为  $\Lambda = \sqrt{\pi R C_{\text{ext}} / f}$ <sup>[31]</sup>,其中  $R$  是 FMF 的包层半径,  $C_{\text{ext}}=5760$  m/s 为声波在石英光纤中的传播速度,  $f$  为加载电信号的频率。当满足模式耦合条件<sup>[32]</sup>:  $\Lambda = L_B = \lambda / (n_{01} - n_{11})$  时  $LP_{01}$  模向  $LP_{11}$  模耦合,其中  $\lambda$  为传输激光波长,  $n_{01}$  和  $n_{11}$  分别为  $LP_{01}$  模和  $LP_{11}$  模的有效折射率。

实验首先搭建系统,测试 AIFG 的模式调控特性。如图 1(a)所示,在宽谱光源之后连接 AIFG,通过射频信号源加载不同频率和幅度的电信号后, AIFG 将特定波长的基模高效地转换为  $LP_{11}$  模。AIFG 输出端连接一段单模光纤(SMF),并将 SMF 以极小的直径盘绕,  $LP_{11}$  模将在 SMF 被损耗,导致宽谱光源的光谱在此波长产生透射峰,由光谱仪(OSA, YOKOGAWA AQ6380)测量。通过对比宽谱光源的原始光谱以及经过 AIFG 后的透射光谱,测得电信号频率与波长透射峰的关系如图 1(b)所示。实验中利用多个不同波段的宽谱放大自发辐射(ASE)光源与超辐射发光二极管(SLD)光源进行测试,使得测试波长覆盖 1000~1700 nm。由图 1(b)可知,通过改变加载信号频率和电压,从 1000~1700 nm 波段透射谱可达到 11~16 dB,表明从  $LP_{01}$  模到  $LP_{11}$  模的转换具有较高的转换效率。

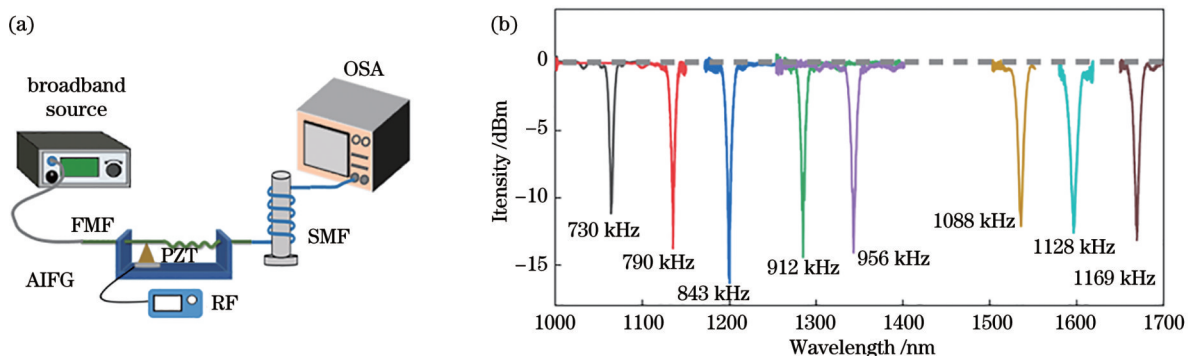


图 1 AIFG 透射谱的测试结构与结果。(a)测试结构;(b)加载不同频率电信号时  $LP_{01}$  模透射谱

Fig. 1 Detecting structure and results of transmission spectra of acoustic-induced fiber grating (AIFG). (a) Schematic diagram of detecting; (b) transmission spectra of  $LP_{01}$  mode at loaded electrical signals of different frequencies

经计算,透射峰波长随着电信号频率线性增加,其关系可拟合为 $\lambda = 1.498f - 87.2$ ,其中波长 $\lambda$ 的单位为 nm,频率 $f$ 的单位为 kHz。当激光输出波长变化时,可通过拟合关系结合光斑图样确定最佳的工作频率。

## 2.2 级联随机拉曼光纤激光器

为实现超宽波长可调谐涡旋光输出,搭建如图 2 所示的级联随机拉曼光纤激光器。采用具备时序稳定特性<sup>[33]</sup>的 ASE 光源作为泵浦源以提高级联转换效率。自制的 ASE 光源输出约 20 mW,其后连接可调谐滤波器(tunable filter)调控中心波长和带宽,中心波长为 1080 nm,带宽约 3 nm。通过两级掺镱放大器将泵浦功率提高到 80 W 以上。由于 ASE 光源对于后向回光较为敏感,采用高功率环形器(最大承受功率为 100 W)对泵浦源进行隔离。本文随机拉曼光纤激光器采用半开腔结构,该半开腔由光纤高反射镜(HR mirror)、拉曼光纤和自制光纤端帽组成。泵浦光通过波分复用器

(WDM, 10/125 光纤)耦合进光纤,反射镜连接在波分复用器的另一端口,可对 1~2  $\mu\text{m}$  的激光均实现高反射率( $>99.5\%$ )。激光输出端帽镀有宽带增透膜以避免端面反馈。由于常规单模光纤在 $\sim 1.32 \mu\text{m}$  的零色散波长处会产生展宽<sup>[34]</sup>,本实验中的拉曼增益光纤采用 500 m 长的商用 CS980 光纤(YOFC CS980-125-20/250),其纤芯直径约为 4  $\mu\text{m}$ ,数值孔径 NA 为 0.24,零色散波长约为 1.82  $\mu\text{m}$ 。由于其纤芯直径较小,WDM 与 CS980 光纤熔接时会出现模场不匹配,通过调整熔接时的放电量和偏移量,可以实现较低损耗熔接。同时,在熔点后端光纤涂覆匹配膏以滤除包层光。AIFG 作为模式调控器件,连接在 CS980 光纤之后,其使用少模阶跃折射率光纤,纤芯直径为 16  $\mu\text{m}$ ,数值孔径 NA 为 0.11,在 1  $\mu\text{m}$  波段支持 4 种 LP 模式,在 1.5  $\mu\text{m}$  波段支持 2 种 LP 模式。在 AIFG 后连接手摇式三环式偏振控制器(PC),以实现输出模场偏振态的调控。

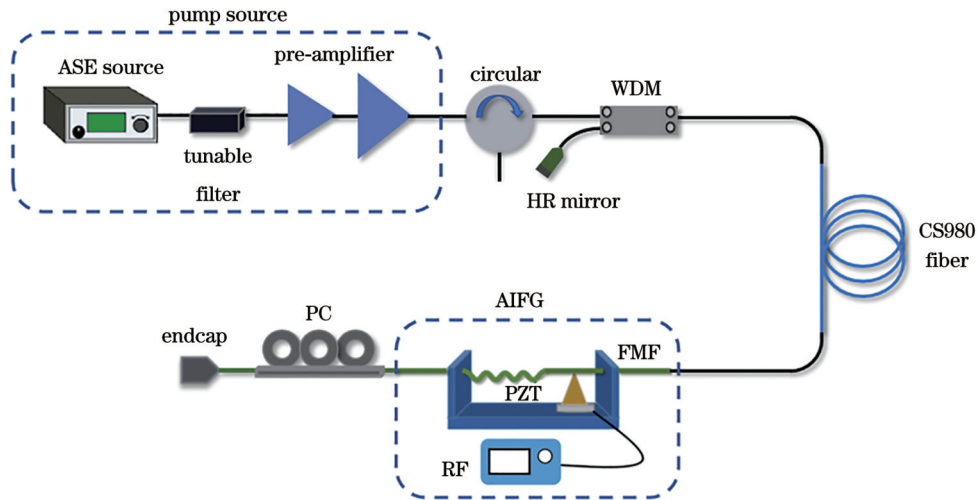


图 2 基于 AIFG 的级联随机拉曼光纤激光器结构示意图

Fig. 2 Structure diagram of cascaded random Raman fiber laser based on AIFG

## 3 实验结果与讨论

### 3.1 级联拉曼光纤激光器输出特性

受激拉曼散射具有明显的阈值特性,当泵浦功率达到拉曼阈值后,泵浦能量开始向拉曼光转移。通过对输出光谱积分,计算得到各阶拉曼光功率变化曲线如图 3(a)所示。随着能量不断积累,当达到下一阶拉曼阈值时,能量依次向下一阶拉曼光转移,每次波长转换满足石英光纤 13.2 THz 的拉曼频移。各阶拉曼光输出功率峰值处的归一化线性光谱如图 3(b)所示。当泵浦功率达到 76 W 时,通过 6 级转换,输出波长达到 1513.7 nm,功率为 23.6 W,总效率为 31.1%。

随着波长转换次数增加,高阶拉曼光的纯度有所降低,其光谱纯度变化如图 3(c)所示,从前两阶拉曼光纯度 $>98.5\%$ 降低到第 6 阶拉曼光纯度 93.4%。各

阶拉曼光相比于泵浦光的转换效率如图 3(d)所示,随着阶次增加,光光效率逐渐降低,从一阶拉曼光的 41.9% 下降至 6 阶拉曼光的 31.1%,其主要原因在于,随着级联阶数增加,每一级能量转换不完全,上一级功率残留导致下一阶拉曼光效率降低。通过调整泵浦功率,可以将输出波长控制在所需要的波段,同时,缩短拉曼光纤长度并提升泵浦功率,可使目标波长输出功率进一步提升。

实验还对激光器输出光谱和功率稳定性进行了测试。图 4(a)展示了输出激光在 10 min 内的功率变化,各阶拉曼光功率波动不超过 5%。光谱稳定性测试中,各阶拉曼光的光谱纯度波动不超过 2%,中心波长偏移 $<0.2 \text{ nm}$ ,图 4(b)展示了中心波长为 1513.7 nm 的 6 阶拉曼光的测试结果。各



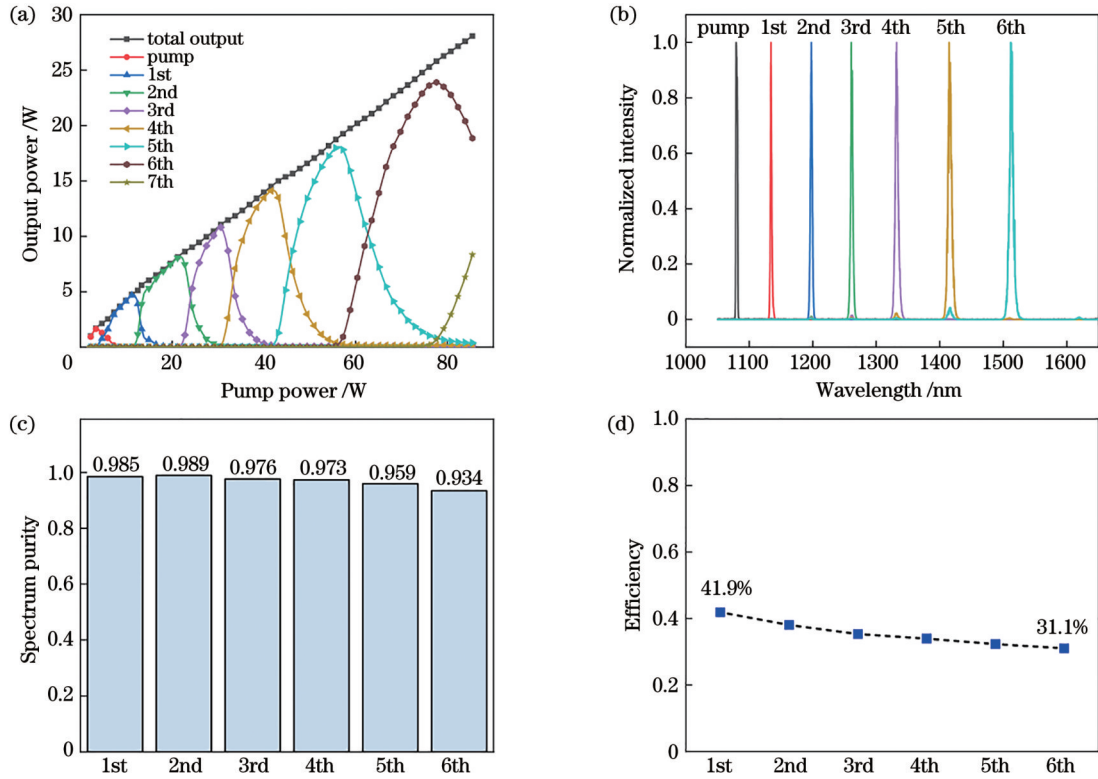


图 3 级联拉曼光纤激光器输出特性实验结果。(a)输出总功率以及各阶拉曼光功率随泵浦光功率变化;(b)各阶拉曼光峰值功率时的归一化线性光谱;(c)各阶拉曼光的光谱纯度;(d)各阶拉曼光效率

Fig. 3 Experimental results of output characteristics of cascade Raman fiber laser. (a) Total output power and inband power of each Raman Stokes as a function of pump power; (b) normalized linear spectrum at peak power of each Raman Stokes; (c) spectral purity of each Raman Stokes; (d) efficiency of each Raman Stokes

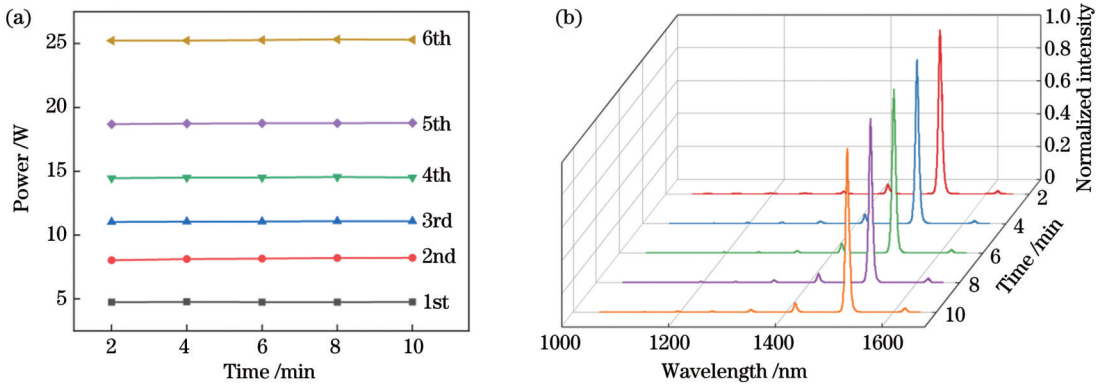


图 4 激光稳定性测试结果。(a)各阶拉曼光的功率波动;(b)第 6 阶拉曼光的归一化光谱稳定性

Fig. 4 Results of laser stability test. (a) Power fluctuation of each Raman Stokes; (b) normalized spectrum stability of the 6<sup>th</sup> Raman Stokes

### 3.2 1.1~1.5 μm 涡旋光输出特性

为实现高性能涡旋随机激光输出,输出端的 AIFG 作为模式调控器件,将产生的各阶拉曼光转换为 LP<sub>11</sub> 模,不同波长处加载的射频信号频率由拟合关系确定。LP<sub>11</sub> 模式由 4 个矢量模式简并而成,通过旋转光纤偏振控制器,当使得光纤中的矢量模式产生  $\pi/2$  相位差时,可以叠加产生拓扑荷为  $l=\pm 1$  的涡旋光束。为检测输出涡旋光的拓扑荷,采取自干涉法<sup>[35]</sup>,

使涡旋光与具有一定横向位移的自身光斑干涉,根据涡旋光自干涉产生的两个分叉点即可判断产生涡旋光的拓扑荷的大小和方向。

本实验搭建如图 5 所示的迈克尔孙自干涉光路。激光由端帽输出后,经焦距为 16 mm 的准直镜准直,准直后的光经 4 个平板玻璃 (flat glass, 反射率约 4%) 反射进行衰减,平板玻璃 1~3 处透射光由经黑色阳极氧化的挡光板进行均匀散射,在第 4 个平板玻璃透射

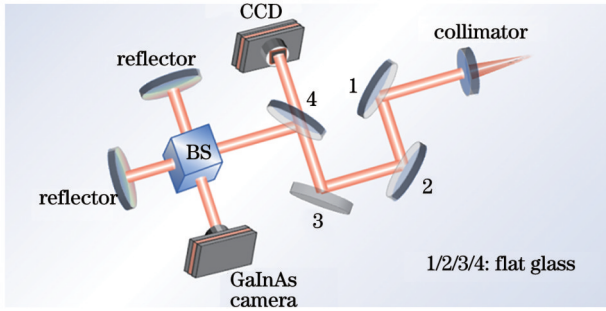


图 5 涡旋随机拉曼光纤激光自干涉结构示意图

Fig. 5 Self-interference setup of vortex random Raman fiber laser

端,利用钢镓砷相机(Xeva-320)采集原始输出光斑。经过两次反射后的光经过一个 50:50 的非偏振分束立方(BS,镀有 1100~1650 nm 增透膜)分成两路,两路光再通过两个相同的宽带介质膜反射镜(reflector,反射率 >99%,工作波长为 1100~1650 nm)原路返回至 BS,并在 BS 的另一端口叠加实现干涉,由钢镓砷相机采集干涉图样。由于随机拉曼激光相干长度较短,因此将两个反射镜放置于精密位移台上,保证两路光的光程差小于相干长度。

各阶拉曼光的原始输出光斑以及自干涉后的光斑图样如图 6 所示。左侧展示了输出的线性光谱,右侧为产生的 LP<sub>11</sub> 模、涡旋光束以及自干涉条纹。采集的

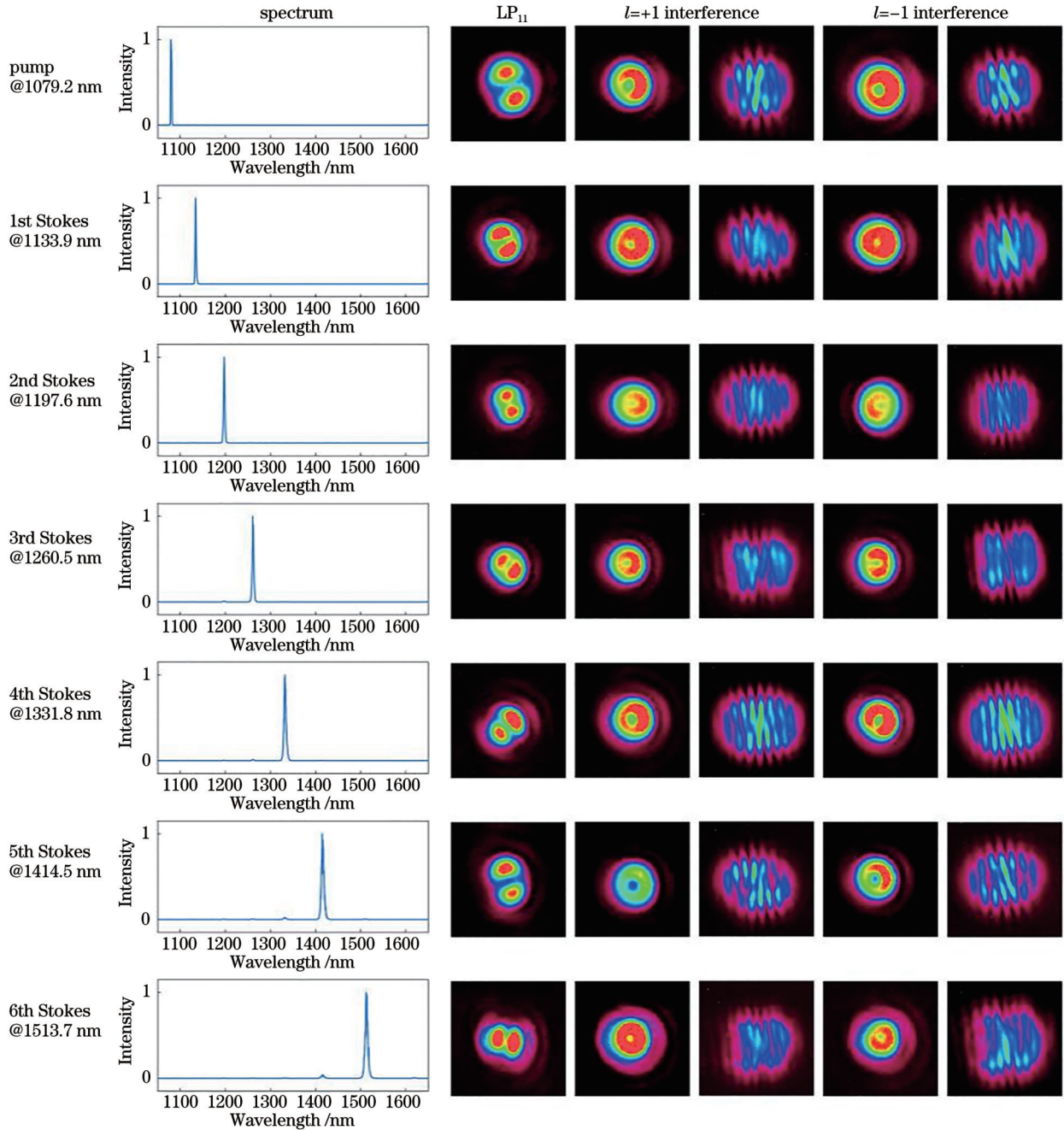


图 6 各阶涡旋随机拉曼光的光谱、原始光斑、LP<sub>11</sub> 模光斑以及自干涉光斑

Fig. 6 Spectrum, original beam profile, LP<sub>11</sub> mode beam profile, and self-interference pattern of each vortex random Raman Stokes

涡旋光光强分布为典型的甜甜圈状分布。由于两路光各有一个相位奇点,自干涉后产生了两个相反方向的“Y”形干涉图样,证明产生了拓扑荷数 $|l|=1$ 的相位涡旋光束。在同一测试条件下,测得对应“Y”形开口方向恰好相反的两个光斑,证明光束相位奇点拓扑荷符号恰好相反,可以证明既产生了 $OAM_{+1}$ ,也产生了 $OAM_{-1}$ 光束。

## 4 结 论

综上所述,本文提出了一种全光纤结构的 $1.1\sim 1.5\ \mu\text{m}$ 波段的高功率涡旋光束随机激光器。基于宽带AIFG与随机激光器的级联拉曼频移,实现了1133.9、1197.6、1260.5、1331.8、1414.5、1513.7 nm波长处拓扑荷数 $l=\pm 1$ 的涡旋光束输出,并通过自干涉实验进行了验证。经过6级拉曼转换,1513.7 nm波长处涡旋光功率为23.6 W,效率为31.1%。AIFG的超宽带模式转换能力,为实现大功率特殊波段涡旋光束提供了可能的技术方案。通过更换泵浦源、增益光纤及相关器件,可将涡旋光束波长覆盖范围进一步扩大到其他波段,并拓展涡旋光在多维光通信、光场与物质相互作用等领域的应用。

## 参 考 文 献

- [1] Zhang J X, Lin Z Z, Liu J, et al. SDM transmission of orbital angular momentum mode channels over a multi-ring-core fibre [J]. *Nanophotonics*, 2022, 11(4): 873-884.
- [2] Shi Y, Blackman D R, Zhu P, et al. Electron pulse train accelerated by a linearly polarized Laguerre-Gaussian laser beam [J]. *High Power Laser Science and Engineering*, 2022, 10: e45.
- [3] Yang Y J, Ren Y X, Chen M Z, et al. Optical trapping with structured light: a review[J]. *Advanced Photonics*, 2021, 3(3): 034001.
- [4] Willig K I, Keller J, Bossi M, et al. STED microscopy resolves nanoparticle assemblies[J]. *New Journal of Physics*, 2006, 8(6): 106.
- [5] Yavorsky M, Vikulin D, Alexeyev C, et al. Photon-phonon spin-orbit interaction in optical fibers[J]. *Optica*, 2021, 8(5): 638-641.
- [6] 吕浩然, 白毅华, 叶紫薇, 等. 利用超表面的涡旋光束产生进展(特邀)[J]. *红外与激光工程*, 2021, 50(9): 20210283.  
Lü H R, Bai Y H, Ye Z W, et al. Generation of optical vortex beams via metasurfaces (Invited) [J]. *Infrared and Laser Engineering*, 2021, 50(9): 20210283.
- [7] 戴茂春, 樊代和, 王尧, 等. 基于空间光调制器的高质量螺旋光束制备[J]. *中国激光*, 2016, 43(9): 0905004.  
Dai M C, Fan D H, Wang Y, et al. Generation of high quality helical beams based on spatial light modulator[J]. *Chinese Journal of Lasers*, 2016, 43(9): 0905004.
- [8] Fridman M, Nixon M, Dubinskii M, et al. Fiber amplification of radially and azimuthally polarized laser light[J]. *Optics Letters*, 2010, 35(9): 1332-1334.
- [9] Gregg P, Mirhosseini M, Rubano A, et al. Q-plates as higher order polarization controllers for orbital angular momentum modes of fiber[J]. *Optics Letters*, 2015, 40(8): 1729-1732.
- [10] Sun B, Wang A T, Xu L X, et al. Low-threshold single-wavelength all-fiber laser generating cylindrical vector beams using a few-mode fiber Bragg grating[J]. *Optics Letters*, 2012, 37(4): 464-466.
- [11] Zhao Y H, Wang T X, Mou C B, et al. All-fiber vortex laser generated with few-mode long-period gratings[J]. *IEEE Photonics Technology Letters*, 2018, 30(8): 752-755.
- [12] Zhao X Y, Liu Y Q, Liu Z Y, et al. Wavelength tunable OAM mode converters based on chiral long-period gratings[J]. *IEEE Photonics Technology Letters*, 2020, 32(24): 1519-1522.
- [13] Lu Y, Liu W G, Chen Z L, et al. Spatial mode control based on photonic lanterns[J]. *Optics Express*, 2021, 29(25): 41788-41797.
- [14] Wang T, Wang F, Shi F, et al. Generation of femtosecond optical vortex beams in all-fiber mode-locked fiber laser using mode selective coupler[J]. *Journal of Lightwave Technology*, 2017, 35(11): 2161-2166.
- [15] Lu J F, Shi F, Meng L H, et al. Real-time observation of vortex mode switching in a narrow-linewidth mode-locked fiber laser[J]. *Photonics Research*, 2020, 8(7): 1203-1212.
- [16] Zhang W D, Huang L G, Wei K Y, et al. High-order optical vortex generation in a few-mode fiber via cascaded acoustically driven vector mode conversion[J]. *Optics Letters*, 2016, 41(21): 5082-5085.
- [17] Zhang W D, Wei K Y, Huang L G, et al. Optical vortex generation with wavelength tunability based on an acoustically-induced fiber grating[J]. *Optics Express*, 2016, 24(17): 19278-19285.
- [18] 李阳, 范晨晨, 郝修路, 等. 高功率涡旋拉曼光纤激光器[J]. *红外与激光工程*, 2023, 52(6): 20230292.  
Li Y, Fan C C, Hao X L, et al. High-power vortex Raman fiber laser[J]. *Infrared and Laser Engineering*, 2023, 52(6): 20230292.
- [19] 刘俊, 王健. 涡旋光激光器研究进展[J]. *中国激光*, 2022, 49(12): 1201001.  
Liu J, Wang J. Research progress of vortex laser[J]. *Chinese Journal of Lasers*, 2022, 49(12): 1201001.
- [20] Long J H, Jin K K, Chen Q, et al. Generating the 1.5 kW mode-tunable fractional vortex beam by a coherent beam combining system[J]. *Optics Letters*, 2023, 48(19): 5021-5024.
- [21] Hou T Y, Chang Q, Chang H X, et al. Structuring orbital angular momentum beams by coherent laser array systems with tip-tilt optimization[J]. *Results in Physics*, 2020, 19: 103602.
- [22] Hu H F, Chen Z, Cao Q, et al. Wavelength-tunable and OAM-switchable ultrafast fiber laser enabled by intracavity polarization control[J]. *IEEE Photonics Journal*, 2023, 15(1): 1500704.
- [23] Dong Z P, Sun H G, Zhang Y M, et al. Visible-wavelength-tunable, vortex-beam fiber laser based on a long-period fiber grating[J]. *IEEE Photonics Technology Letters*, 2021, 33(21): 1173-1176.
- [24] Gui L L, Wang C S, Ding F, et al. 60 nm span wavelength-tunable vortex fiber laser with intracavity plasmon metasurfaces [J]. *ACS Photonics*, 2023, 10(3): 623-631.
- [25] 周朴, 姚天甫, 范晨晨, 等. 拉曼光纤激光: 50年的历程、现状与趋势(特邀)[J]. *红外与激光工程*, 2022, 51(1): 20220015.  
Zhou P, Yao T F, Fan C C, et al. 50th anniversary of Raman fiber laser: history, progress and prospect (Invited)[J]. *Infrared and Laser Engineering*, 2022, 51(1): 20220015.
- [26] Wu J D, Lai Z, Zhou Y, et al. High energy singular beams generation from a dissipative soliton resonance Raman fiber laser [J]. *Journal of Lightwave Technology*, 2023, 41(15): 5091-5096.
- [27] Turitsyn S K, Babin S A, El-Taher A E, et al. Random distributed feedback fibre laser[J]. *Nature Photonics*, 2010, 4: 231-235.
- [28] Ye J, Ma X Y, Zhang Y, et al. Revealing the dynamics of intensity fluctuation transfer in a random Raman fiber laser[J]. *Photonics Research*, 2022, 10(3): 618-627.
- [29] Ma X Y, Ye J, Zhang Y, et al. Vortex random fiber laser with controllable orbital angular momentum mode[J]. *Photonics Research*, 2021, 9(2): 266-271.
- [30] Luo K H, Ma R, Wu H, et al. Flexible generation of broadly wavelength- and OAM-tunable Laguerre-Gaussian (LG) modes



- from a random fiber laser[J]. *Optics Express*, 2023, 31(19): 30639-30649.
- [31] Blake J N, Kim B Y, Engan H E, et al. Analysis of intermodal coupling in a two-mode fiber with periodic microbends[J]. *Optics Letters*, 1987, 12(4): 281-283.
- [32] Vengsarkar A M, Pedrazzani J R, Judkins J B, et al. Long-period fiber-grating-based gain equalizers[J]. *Optics Letters*, 1996, 21(5): 336-338.
- [33] Yao T F, Chen Y Z, Zhang Y, et al. All-fiberized cascaded random Raman fiber laser with high spectral purity based on filtering feedback[J]. *Applied Optics*, 2019, 58(35): 9728-9733.
- [34] Zhang Y, Xu J M, Ye J, et al. Cascaded telecom fiber enabled high-order random fiber laser beyond zero-dispersion wavelength [J]. *Optics Letters*, 2020, 45(15): 4180-4183.
- [35] Lan B, Liu C, Rui D M, et al. The topological charge measurement of the vortex beam based on dislocation self-reference interferometry[J]. *Physica Scripta*, 2019, 94(5): 055502.

## 1.1–1.5 $\mu\text{m}$ Waveband High Power Random Vortex Beams Based on Acoustically-Induced Fiber Grating

Li Yang<sup>1</sup>, Yao Tianfu<sup>1,2,3\*</sup>, Fan Chenchen<sup>1</sup>, Hao Xiulu<sup>1</sup>, Ma Xiaoya<sup>1</sup>, Xu Jiangming<sup>1</sup>, Zhang Qingsong<sup>4</sup>, Zeng Xianglong<sup>4\*\*</sup>, Zhou Pu<sup>1</sup>

<sup>1</sup>College of Advanced Interdisciplinary Studies, National University of Defense Technology, Changsha 410073, Hunan, China;

<sup>2</sup>Nanhu Laser Laboratory, National University of Defense Technology, Changsha 410073, Hunan, China;

<sup>3</sup>Hunan Provincial Key Laboratory of High Energy Laser Technology, Changsha 410073, Hunan, China;

<sup>4</sup>Key Laboratory of Specialty Fiber Optics and Optical Access Networks, Joint International Research Laboratory of Specialty Fiber Optics and Advanced Communication, Shanghai University, Shanghai 200444, China

### Abstract

**Objective** In recent years, vortex beams carrying orbital angular momentum (OAM) have caught much attention due to their research significance and application prospects. With the applications of vortex beams in sensing, measurement, and high-capacity optical communication, the output bandwidth and wavelength tunability of vortex beams have become a research focus. Breaking through the emission wavelength limitation of rare-earth doped fiber, and the device of broadband mode conversion is the basis for realizing the output of special band/broadband vortex light. Currently, many devices can realize vortex beam output in a fiber laser. However, most devices are designed and manufactured according to the target wavelength. The acoustically-induced fiber grating (AIFG) achieves mode conversion by acousto-optic coupling in passive fibers. When the operating wavelength changes, it only needs to change the frequency of the loaded electric signal, without re-designing and replacing the parameters of the mode conversion device. Theoretically, it has an extremely wide operating bandwidth. Considering the above requirements, the structure of random Raman fiber laser (RRFL) based on distributed Rayleigh backscattering is adopted to realize broadband vortex beams by combining the AIFG.

**Methods** By combining the AIFG and RRFL, when the output wavelength is converted by Raman frequency shift, there is no need to redesign and replace the mode conversion device. The transmission spectrum of the  $LP_{01}$  mode is tested in Fig. 1(b), which indicates that there is a high efficiency of mode conversion from 1000 to 1700 nm. The RRFL is built as shown in Fig. 2. An amplified spontaneous emission (ASE) source including two amplification stages is utilized as the pump source which is then coupled into the half-open cavity of RRFL by wavelength division multiplexing (WDM). The half-open cavity is formed by a high-reflective (HR) optical fiber mirror which is attached to the WDM, a piece of gain fiber, and a homemade fiber endcap. The reflectance of the HR mirror is more than 99.5% at 1–2  $\mu\text{m}$ , and anti-reflection coating is conducted on the endcap to evade unwanted end feedback. The gain fiber is the commercial CS980 fiber with a length of 500 m. Once the suitable electrical signal is loaded on the AIFG, the output mode is converted to  $LP_{11}$  mode, and the ring-shaped radially polarized light and vortex beam with topological charge  $l = \pm 1$  output can be realized by precise polarization control.

**Results and Discussions** When the pump power reaches the Raman threshold, the pump energy begins to transfer to the Raman Stokes. By integrating the output spectrum, the variation curves of the Raman optical power of each order are calculated, as shown in Fig. 3(a). When the pump power reaches 76 W, the output wavelength reaches 1513.7 nm by the six-stage Raman shift, with a power of 23.6 W and a total efficiency of 31.1%. With the cascaded wavelength conversion,

the purity and efficiency of high-order Raman light decrease, which is shown in Figs. 3(c) and 3(d). With the increasing output wavelength, the loss of gain fiber rises with the incomplete conversion of each stage, which results in a gradual efficiency decrease. Once there is a  $\pi/2$  phase difference between the eigenmodes by controlling the polarization controller (PC), the vortex beam can be realized via the superposition of the two modes, and the “Y-shaped” interference fringe can be detected by the self-interference experiment (Fig. 5), which proves that the vortex beam with topological charge  $l=\pm 1$  is generated.

**Conclusions** We propose an all-fiber high-power RRFL with vortex beam output in the 1.1–1.5  $\mu\text{m}$  band. Based on the cascaded Raman shift and broadband AIFG, the output of vortex beams with topological charges  $l=\pm 1$  at 1133.9, 1197.6, 1260.5, 1331.8, 1414.5, and 1513.7 nm wavelengths is realized, and the topological charge is verified by self-interference experiments. After the six-stage conversion, the power at 1513.7 nm wavelength is 23.6 W, with an efficiency of 31.1%. The ultra-wide wavelength tuning capability of the AIFG is expected to make it a key device to fill the spectral gap of vortex beams and can provide a reliable light source for the application of special wavelength vortex beams. By replacing the pump source, gain fiber, and related devices, the wavelength coverage of the vortex beam can be further expanded in other wavebands, and the application of vortex light in multi-dimensional optical communication and interaction between light field and matter can be further expanded.

**Key words** random Raman fiber laser; vortex beam; acoustically-induced fiber grating; orbital angular momentum